Hindawi
Geofluids
Volume 2021, Article ID 5536235, 14 pages
https://doi.org/10.1155/2021/5536235

Research Article

Design of Longwall Coal Pillar for the Prevention of Water Inrush from the Seam Floor with Through Fault

Ang Li[1,2] **Bing nan Ji**[1] **Qiang Ma**[3] **Chaoyang Liu**[4] **Feng Wang**[4] **Li Ma**[2] **Pengfei Mu**[3] **Lin Mou**[3] **Yuxuan Yang**[1] **and Xuesong Ding**[1]

[1]*School of Architecture and Civil Engineering, Xi'an University of Science and Technology, Xi'an, Shaanxi 710054, China*
[2]*Key Laboratory of Coal Resources Exploration and Comprehensive Utilization, Ministry of Land and Resources, Xi'an, Shaanxi 710021, China*
[3]*Xi'an Research Institute of China Coal Technology & Engineering Group Corp, Xi'an, Shaanxi 710077, China*
[4]*Shaanxi Coal Chemical Industry Group Chenghe Mines Co., Ltd., Weinan Shaanxi 715200, China*

Correspondence should be addressed to Ang Li; ang.li3399@gmail.com

Received 22 January 2021; Accepted 23 June 2021; Published 22 July 2021

Academic Editor: Dayang Xuan

Copyright © 2021 Ang Li et al. This is an open access article distributed under the Creative Commons Attribution License, which permits unrestricted use, distribution, and reproduction in any medium, provided the original work is properly cited.

Setting up a waterproof coal pillar is an important measure to prevent water inrush from the Weibei mining through fault floor. Based on the plastic slip line field theory, a mechanical model of floor water inrush induced by confined water in the through fault zone was established. The mechanical expressions of confined water pressure and the width of the waterproof coal pillar under the state of limit equilibrium were derived. Combining the laws of floor deformation, failure and fault activation under two kinds of coal pillar width, the safety width of the waterproof coal pillar was determined. Furthermore, the safety threshold is better than the empirical value mentioned in the "coal mine safety regulations." Following this, grouting transformation was carried out on the K2 sand layer of the cut roadway floor. This provided a theoretical basis and engineering practice for water disaster prevention and the control of the structural floor under similar conditions in the Weibei mining area for future benefit.

1. Introduction

The North China-type coalfield is rich in coal resources and accounts for about 90% of the total coal [1, 2]. However, the complex hydrogeological conditions of minefields have caused the frequent occurrence of limestone karst water hazards [2, 3]. With the large-scale development of coal resources in the recent decades, the shallow North China-type coalfield has gradually entered the stage of deep mining and lower group coal mining [4, 5]. Furthermore, the coal seam floor is increasingly threatened by Ordovician ash highly confined water [6–8].

In some old mining areas, coal reserves threatened by karst water disasters account for 49%-87.6% of total mine reserves [9]. The Carboniferous-Permian coalfield in Weibei, known as the "Weibei black belt," is distributed in Tongchuan, Pubai, Chenghe, and Hancheng mining areas. Faults on the floor generally exist in the geological structure of the Weibei coalfield. Once mining induces fault activation, Ordovician confined water can easily rise along the fault zone and connected fractures. This results in water inrush from the floor.

Currently, remarkable theory and practice bases have been achieved by research carried out on the failure law, water inrush mechanism, and water inrush prediction [10–18]. Yin et al. [19] developed a numerical model to predict the time and the longwall locations of flood occurrences. Furthermore, Odintsev and Miletenko [20] studied the mine water inrush caused by spontaneous hydrofracturing of surrounding rocks and gave the influencing factors of spontaneous hydraulic fracturing. Additionally, Wang et al. [21] established an evaluation model for predicting water inrush in the Lu-an mining area based on fractal theory and improved the analytic hierarchy progress. This model provided a basis for water inrush research from the floor strata through faults. However, the study on the mechanism of water inrush and seepage from the through fault floor in the Weibei mining area has not yet taken a corresponding karst confined water prevention

technology system and supporting measures. In the case of lower group coal resources through fault floors being blindly exploited, it is very easy for floor water inrush to proceed, endangering the safety of the construction of the mine and personnel safety.

The primary floor water inrush prevention and control measures include grouting transformation, water exploration, drainage, and setting of waterproof coal pillars [22–27]. Setting waterproof coal pillar measures is often adopted to prevent water inrush from the Weibei coal mine floor. However, the setting width of the waterproof coal pillar obtained from the empirical formula in "coal mine safety regulations" failed to consider the fault structure with complex conditions. Therefore, scientifically setting up a reasonable width of a waterproof coal pillar is one of the urgent problems to be solved through fault coal seam mining.

This paper established a mechanical model of floor water inrush induced by confined water in the through fault zone. Furthermore, this paper gave an analytical solution of the limit width of the waterproof coal pillar. By combining analysis of the floor's deformation, failure, and the law of fault activation under two kinds of coal pillar width with engineering examples and numerical simulation, it is proven that the mechanical model is reasonable. Moreover, the grouting of floor K2 sandstone can also be used as a reference for the treatment of other similar geological structures.

2. Theoretical Analysis

2.1. Analysis of the Mechanical Model of the Plastic Slip Line. Figure 1 shows the abutment pressure distribution curve of coal in front of the working face. According to the failure degree, the coal body of the working face can be divided into the inelastic zone, the elastic zone, and the original rock stress zone under abutment pressure with the coal seam mining. Among them, the width of the inelastic zone is [28]

$$x_0 = \frac{H_2}{\theta}\left\{\left[\left(krH_1 + \frac{c_1}{f_1} - \sigma_c + \sigma_c^*\right)\left(\frac{f_1}{c_1 + f_1\sigma_c^*}\right)\right]^{\theta/2kpf_1} - 1\right\}, \tag{1}$$

where H_1 is the buried depth of the coal seam (m), H_2 is the mining height of the coal seam (m), k is the peak coefficient of abutment pressure, r is the average bulk density of the coal seam overlying rock (N/m^3), θ is the deformation angle of the coal seam (degree), C_1 is the cohesive force on the contact surface between the coal seam and the roof and floor (MPa),f_1 is the frictional force between the interface between the coal seam and the roof, $k_p = (1 + \sin\varphi_2)/(1 - \sin\varphi_2)$, σ_c is the ultimate compressive strength of the coal under uniaxial compression (MPa), and σ_c^* is the strength of the coal under uniaxial compression residual strength (MPa).

Figure 2 shows the mechanical model of the plastic slip line for mining failure of floor rock mass caused by abutment pressure in front of the coal mining face [29], where O is the coal mining face position, OD is the goaf boundary, OA is the horizontal distance from the peak abutment pressure to the working face, and EF represents the maximum depth of mining failure of the floor. With the advancement of the working face, the maximum failure depth of floor mining is

$$\overline{EF} = \frac{x_0\cos\varphi_d}{2\cos\left((\pi/4) + (\varphi_d/2)\right)} e^{\left(\frac{\pi}{4} + \frac{\varphi_d}{2}\right)\tan\varphi_d}. \tag{2}$$

The horizontal distance between the maximum failure depth $\overline{OE}$ of the floor rock mass and the front end of the work is

$$\overline{0E} = \frac{x_0\sin\varphi_d}{2\cos\left((\pi/4) + (\varphi_d/2)\right)} e^{\left(\frac{\pi}{4} + \frac{\varphi_d}{2}\right)\tan\varphi_d}. \tag{3}$$

The maximum failure length of floor rock mass in the goaf along the horizontal plane is

$$\overline{0D} = \overline{0E} + \overline{ED}, \tag{4}$$

$$\overline{ED} = x_0\tan\left(\frac{\pi}{4} + \frac{\varphi_d}{2}\right)\tan\varphi_d, \tag{5}$$

where x_0 is the width of the inelastic zone of the coal seam (m) and φ_d is the weighted average internal friction angle of the floor rock mass.

2.2. Mechanical Analysis of the Activated Fault Floor Structure. As the dip angle of the through fault is generally large in the Weibei mining area, this paper only discussed the fault with a large dip angle. For the convenience of derivation, the shaping slip line of the base plate is simplified to a straight line, as shown in Figure 3. Then, the angle between shaping slip line and coal seam can be expressed as

$$\beta = \arctan\frac{\overline{EF}}{\overline{OE} + x_0}. \tag{6}$$

The mechanical model in Figure 4 is taken from the triangular region in Figure 3. By analyzing the force of the triangular HGM rock block above fault, the upper rock mass pressure and confined water pressure of the rock block are regarded as a uniformly distributed load, as shown in Figure 4. Among them, q represents the confined water pressure, q_1 represents the uniformly distributed load of the upper rock mass acting on the rock block, and τ_1, σ_1 represent the shear stress and normal stress provided by the lateral rock mass, respectively. The length of each segment can be expressed as

$$\begin{cases} L_1 = \dfrac{\overline{EF}}{\sin\beta}, \\ L_2 = \dfrac{L_1}{\cos(\alpha - \beta)}, \\ L_3 = L_1 \cdot \tan(\alpha - \beta). \end{cases} \tag{7}$$

By decomposing the forces in the diagram, the simplified force expression in the y-axis direction in the limit equilibrium state is

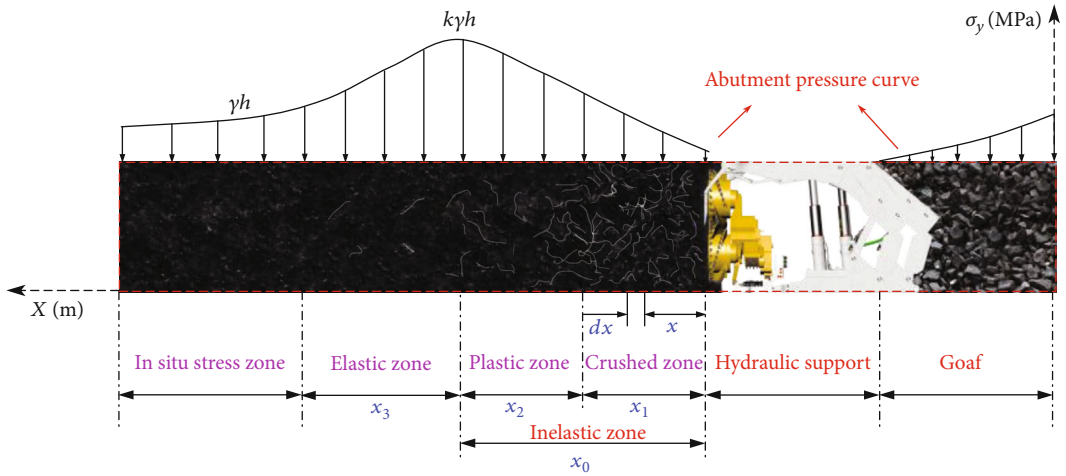

Figure 1: Coal abutment pressure distribution law in front of the working face.

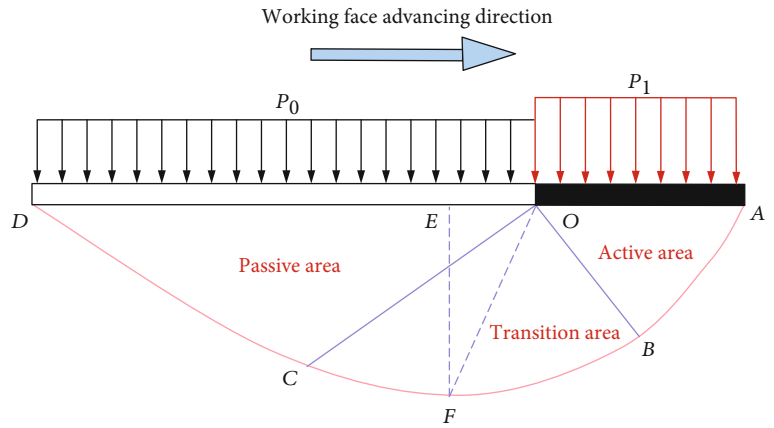

Figure 2: Mechanical model of slip line for floor mining failure.

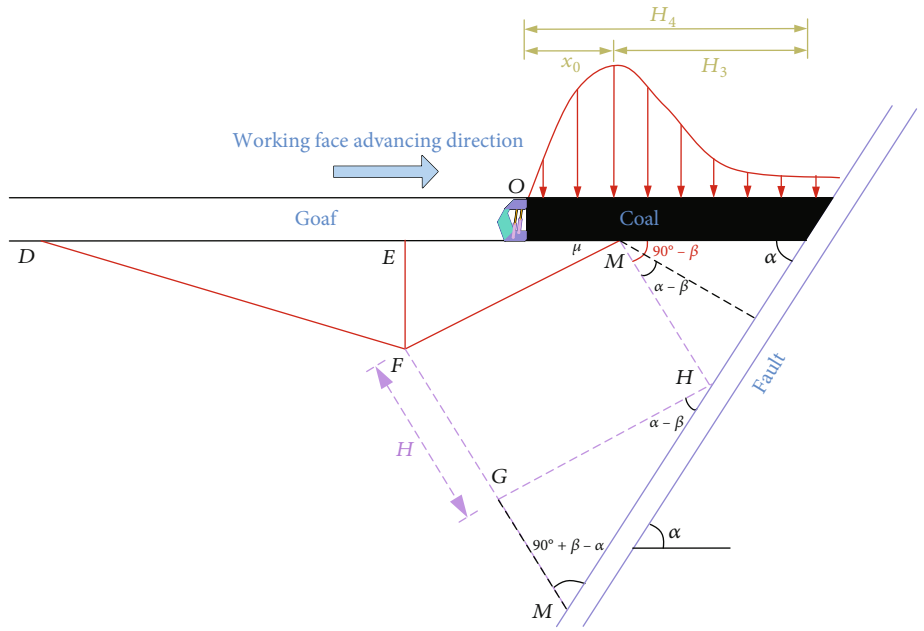

Figure 3: Plane stress analysis of the floor with fault.

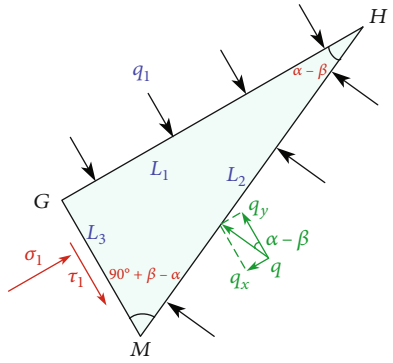

Figure 4: Local stress analysis of triangular rock mass.

$$q_1 = \frac{qL_1 - (\sigma_1 \tan \varphi_d + c_d) \cdot L_3}{L_1}, \tag{8}$$

where C_d is the weighted average cohesion of floor rock mass.

The mechanical model in Figure 5 is taken from the rectangular area in Figure 3. The force of rectangular MFGH rock above the triangle is analyzed, as shown in Figure 5. By taking any microelement d_z in the z-axis direction, the expression of force acting on the z-axis in the equilibrium state is

$$(\sigma_z + d\sigma_z)L_1 - \sigma_z \cdot L_1 - 2(\tau_2 + \tau_3)d_z = 0, \tag{9}$$

$$\tau_2 = \tau_3 = c_d + \sigma_x \cdot \tan \varphi_d, \tag{10}$$

where σ_x is the stress of the element in the x-axis direction (MPa).

Since the failure of the floor rock mass should conform to the principle of shear failure, the M-C criterion is selected as the yield criterion, and the limit ultimate equilibrium condition of the rock mass when it is about to fail is

$$\frac{1 + \sin \varphi_d}{1 - \sin \varphi_d} = \frac{\sigma_z + c \cdot \cot \varphi_d}{\sigma_x + c \cdot \cot \varphi_d}. \tag{11}$$

Let $(1 + \sin \varphi_d)/(1 - \sin \varphi_d) = \lambda$; then,

$$\sigma_x = \frac{\sigma_z + (1 - \lambda) \cdot c_d \cdot \cot \varphi_d}{\lambda}. \tag{12}$$

Substituting formulas (9) and (10) into formula (12), then solving the differential equation, and simplifying, one can obtain

$$\sigma_z = A_1 e^{2z \tan \varphi_d / \lambda L_1} - c_d \cdot \cot \varphi_d \quad (A \text{ is any parameter}). \tag{13}$$

When $z = 0$, take the unit thickness as b. The following formula can be obtained:

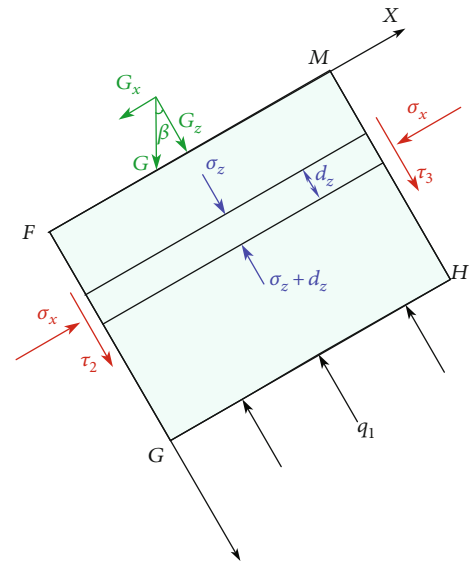

Figure 5: Force analysis of microunit.

$$\sigma_z = \sigma_{G_z} = \frac{1/2\overline{EF} \times \left(\overline{DE} + \overline{EO} + \overline{OM}\right) \times r_1 \times b \times \cos \beta}{L_1 \times b}, \tag{14}$$

where r_1 is the average bulk density of the floor strata (kN/m^3).

The $z = 0$ and formula (14) are substituted into formula (15) and simplified as

$$A_1 = \sigma_z + c_d \cdot \cot \varphi_d. \tag{15}$$

Substituting equation (15) into the differential equation (13), we can get

$$\sigma_z = \left(\frac{r_1 \cos \beta \times S_{\Delta DFM}}{L_1} + c_d \cdot \cot \varphi_d\right) \cdot e^{2z \tan \varphi_d / \lambda L_{11}} - c_d \cdot \cot \varphi_d. \tag{16}$$

By substituting $z = 0$ into equation (16) and taking unit thickness as b, the simplified expression is

$$\sigma_z = q_1 - H \cdot r_1 \cdot \cos \beta. \tag{17}$$

Substituting equation (16) into equation (17), one can obtain

$$q_1 - H \cdot r_1 \cdot \cos \beta = \left(\frac{r_1 \cos \beta \times S_{\Delta DFM}}{L_1} + c_d \cdot \cot \varphi_d\right) \cdot e^{2H \tan \varphi_d / \lambda L_1} - c_d \cot \varphi_d. \tag{18}$$

In this limit state, H can be expressed as

$$H = \frac{H_3 \cdot \sin \alpha}{\cos (\alpha - \beta)}, \tag{19}$$

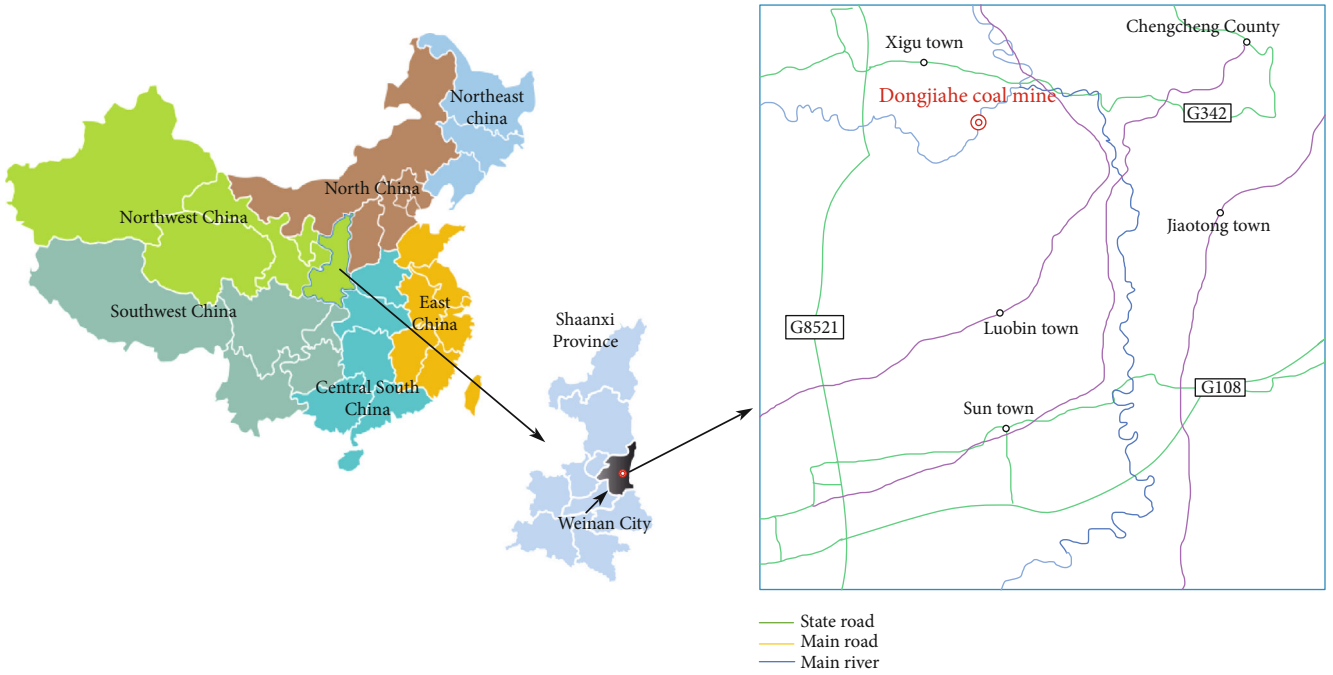

Figure 6: Location of the Dongjiahe coal mine.

where H is the width of the coal pillar corresponding to the direction of the working face (m).

By substituting equations (8) and (19) into equation (18) and simplifying it, the expression of the confined water pressure of the through fault floor and the width of the corresponding coal pillar under the limit equilibrium state can be obtained:

$$q = \frac{(\sigma_1 \cdot \tan \varphi_d + c_d) \cdot L_3 - c_d \cdot L_1 \cdot \cot \varphi_d}{L_1} + \frac{r \cdot \cos \beta \cdot S_{\Delta DFM} + c_d \cdot L_1 \cdot \cot \varphi_d}{L_1} \cdot e^{2H_3 \cdot \sin \alpha \cdot \tan \varphi_d / \lambda L_1 \cdot \cos(\alpha - \beta)} + \frac{r_1 \cdot H_3 \cdot \cos \beta \cdot \sin \alpha}{\cos(\alpha - \beta)}, \tag{20}$$

because this equation is transcendental and cannot be simplified to the $H_3 = f(q)$ form manually. However, it can be given a value by the method of a single variable solution by software. Therefore, the width of waterproof coal pillar H_4 in the through fault floor is

$$H_4 = x_0 + f(q). \tag{21}$$

3. Engineering Practice and Application

3.1. Working Face Overview. The Dongjiahe coal mine is located 3.5 kilometers southwest of Chengcheng County, Weinan City, Shaanxi Province. This mine has a high terrain in the north and low terrain in the south (Figure 6). It belongs to the Weibei Loess Plateau in geomorphology. The main coal seam of the mine is the no. 5 coal, which has a coal thickness of 2.9 m~4.7 m; the dip angle of the coal seam is 3°~15°. The 23503 working face is located in the second level and third mining area of the Dongjiahe coal mine, with a strike length of 1190 m and a dip length of 180 m. The terrain is lower than the static water level of Ordovician ash +370 m. This is classified as mining under pressure.

The 23503 working face is near the eastern boundary of the mining area. It is only about 150 m away from the normal fault of Dongjiahe, which is a big fault outside the minefield. According to drilling, the floor fault structure of the working face is well developed, and the hydrogeological conditions are complex. The distance between the 5# coal seam floor and the top face of the Ordovician limestone is about 62.82 m (CH187)~31.47 m (DB6). There is a normal fault structure on the right boundary of the working face. This fault structure has a fault dip angle of 40°, and the fault crosses the K2 limestone. If mining starts at the working face, mining disturbances would affect the normal fault and result in fracture conduction. This will then cause floor water inrush. Therefore, in the mine, we decided to reduce the disturbance to the fault by setting up a waterproof coal pillar to avoid safety accidents.

3.2. Calculation of Setting Width of the Fault Coal Pillar

3.2.1. Empirical Formula of "Coal Mine Safety Regulations." In the "provisions on prevention and control of water in coal mine," when considering the pressure of fault water along the direction of the coal seam, the width of the waterproof coal pillar can be calculated by referring to the following empirical formula. This calculation applies in the case whereby coal seam is located above the aquifer and the fault is water-conducting.

Table 1: Basic parameters.

H_1 (m)	r (kN/m^3∗10^{-3})	H_2 (m)	K	θ (°)	C_1 (MPa)	f_1	C_d (MPa)	α (°)	q (MPa)
450	0.0215	3.8	5	2	0.25	0.2	2	40	1.4

Table 2: Physical and mechanical parameters of part of rock in the 23503 working face.

Rock stratum	Thickness (m)	Elastic modulus E (MPa)	Tensile strength f_c (MPa)	Friction angle φ (°)	Poisson ratio μ	Volumetric weight γ (kg·m^{-3})
Siltstone	7	8800	4.5	26	0.24	2500
Medium sandstone	10	8500	2.9	28	0.26	2450
Sandy mudstone	1	2850	0.7	32	0.33	2200
No. 5 coal	4	1650	0.8	36	0.32	1500
Siltstone	1	8650	4.3	26	0.25	2460
Quartz sandstone	3	8850	4.8	25	0.24	2650
Sandy mudstone	1	3500	0.7	33	0.34	2250
Siltstone	6	8600	3.3	28	0.24	2530
Quartz sandstone	12	8850	3.7	26	0.25	2650
Siltstone	1	8750	3.9	27	0.24	2550
Quartz sandstone	3	8850	3.7	26	0.25	2650
No. 10 coal	3	2000	0.8	38	0.33	1520
Sandy mudstone	1	2870	0.8	32	0.34	2200
Aluminous mudstone	9	2800	0.7	35	0.35	2050
Ordovician limestone	12	10000	8.0	30	0.26	2600

$$L = 0.5KM\sqrt{\frac{3P}{K_p}} \geq 20\ \text{m}, \tag{22}$$

where L is the width of the coal pillar (m), M is the mining height (m), P is the hydrostatic pressure (MPa), K_p is the tensile strength of coal (MPa), and K is the safety factor; take 2-5.

Substitute the geological parameters of the 23503 working face in the Dongjiahe coal mine into the empirical formula (22), where the basic parameters are as follows: M is 3.8 m, K is 5, K_p is 0.25 MPa, P is 1.4 MPa, and the minimum width of the waterproof coal pillar is 25 m.

3.2.2. Theoretical Solution of the Setting Width of the Waterproof Coal Pillar. Based on the theoretical derivation in the previous section, the mechanical expressions of the confined water pressure with fault floor and the width of the retained waterproof coal pillar were obtained. By substituting the basic parameters of the 23503 working face in Table 1 into formulas (20) and (21), the minimum width theoretical solution of the waterproof coal pillar is 31.92 m.

In summary, the empirical and theoretical values of the waterproof coal pillar width in the 23503 working face were 25.13 m and 31.92 m, respectively. The empirical value was smaller than the theoretical value. Considering that some folds and small fault structures may exist in the actual mining of the working face, there will be unsafe factors in the empirical value of the regulations. Hence, in the mine, we initially proposed to set up a waterproof coal pillar of 28 m. To make a comprehensive study and judgment of the above results, a numerical simulation analysis was carried out on the lower cut mining at the distance of 28 m from the fault.

4. Numerical Simulation

4.1. Numerical Simulation Study on 28 m Width of the Waterproof Coal Pillar

4.1.1. Model Building. Taking the 23503 working face of the Dongjiahe coal mine as a research object and taking the simulated mining depth as 450 m, the mining height as 4.0 m, and the near-horizontal coal seam mining, the size of the model length × width × height is 550 m × 15 m × 170 m. According to the actual lithology of typical drilled columnar strata in the 23503 working face, it was divided into 23 layers of model materials. The fault cut through the coal seam and floor aquifer and entered the Ordovician limestone aquifer. Table 2 shows some rock physical and mechanical parameters of the 23503 working face.

4.1.2. Boundary Conditions and Excavation Steps. The uniformly distributed load was applied at the top of the model to replace unsimulated overburden pressure. Water pressure

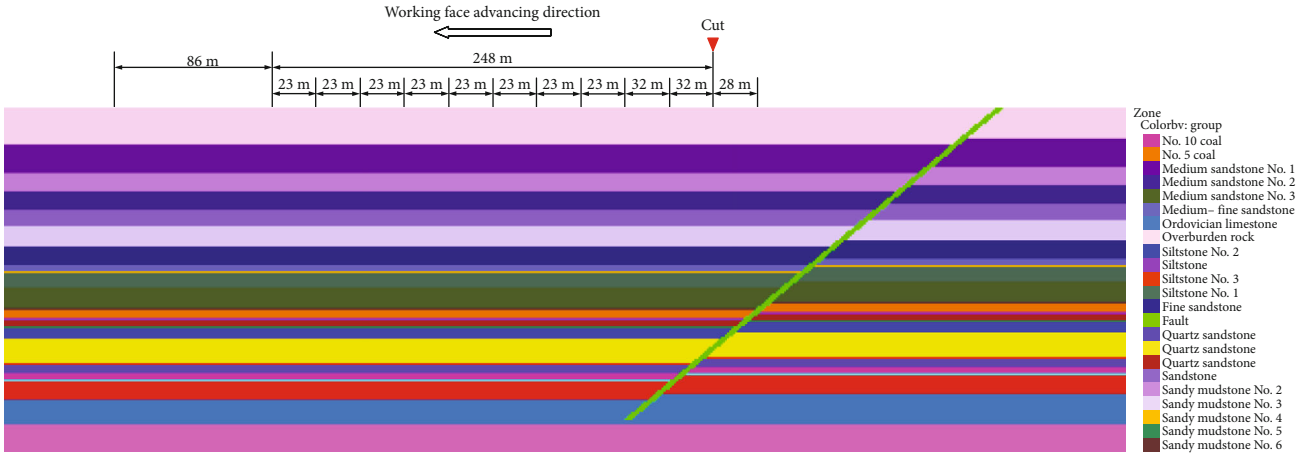

Figure 7: Working face mining schematic diagram.

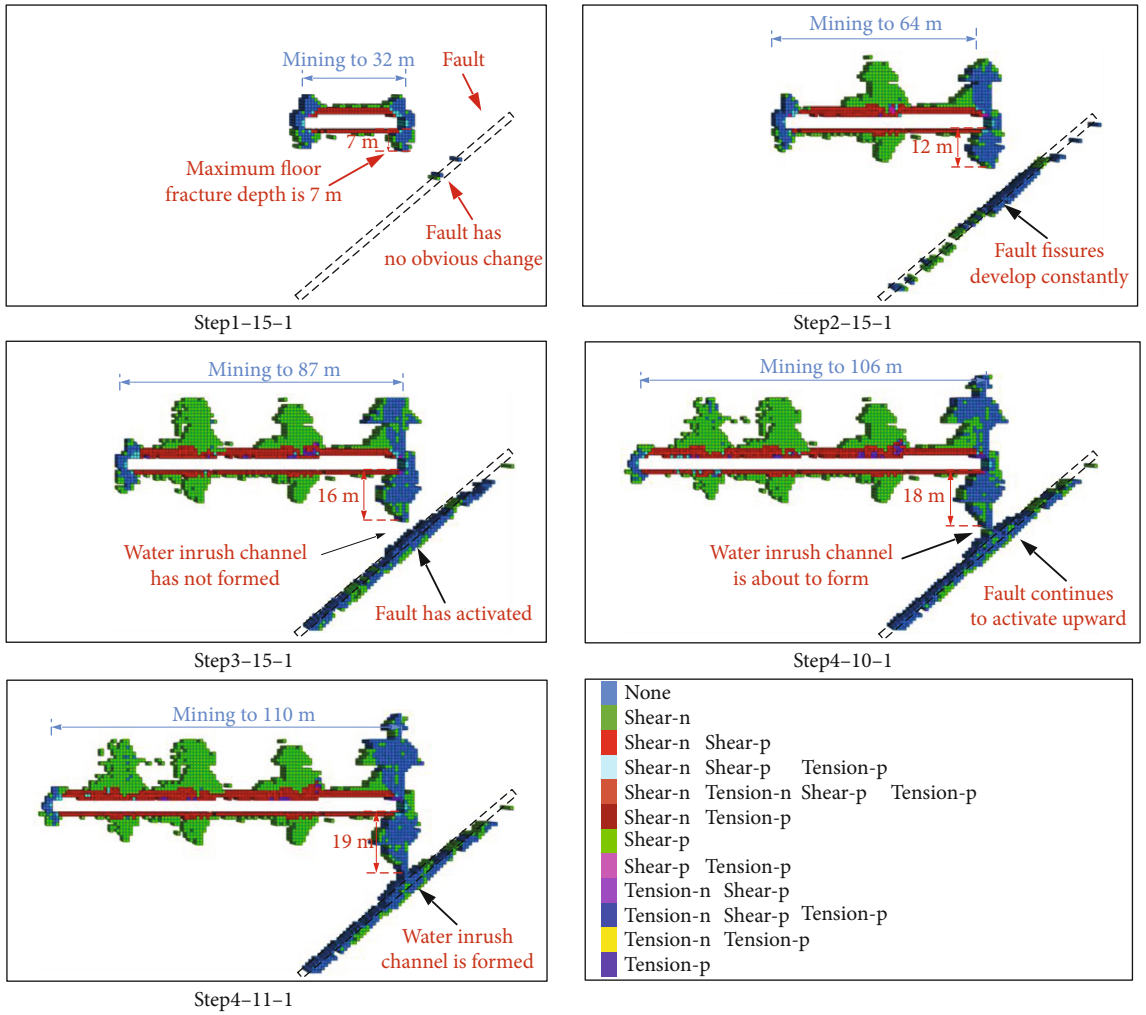

Figure 8: Plastic zone evolution law diagram.

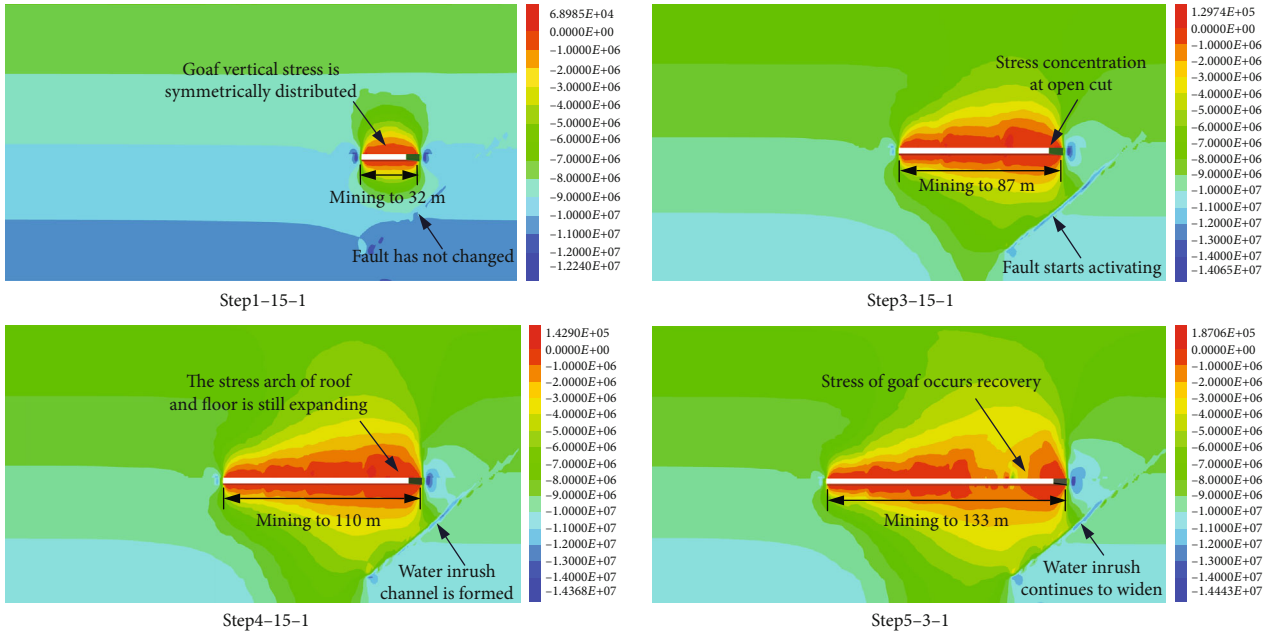

Figure 9: Stress field evolution law diagram.

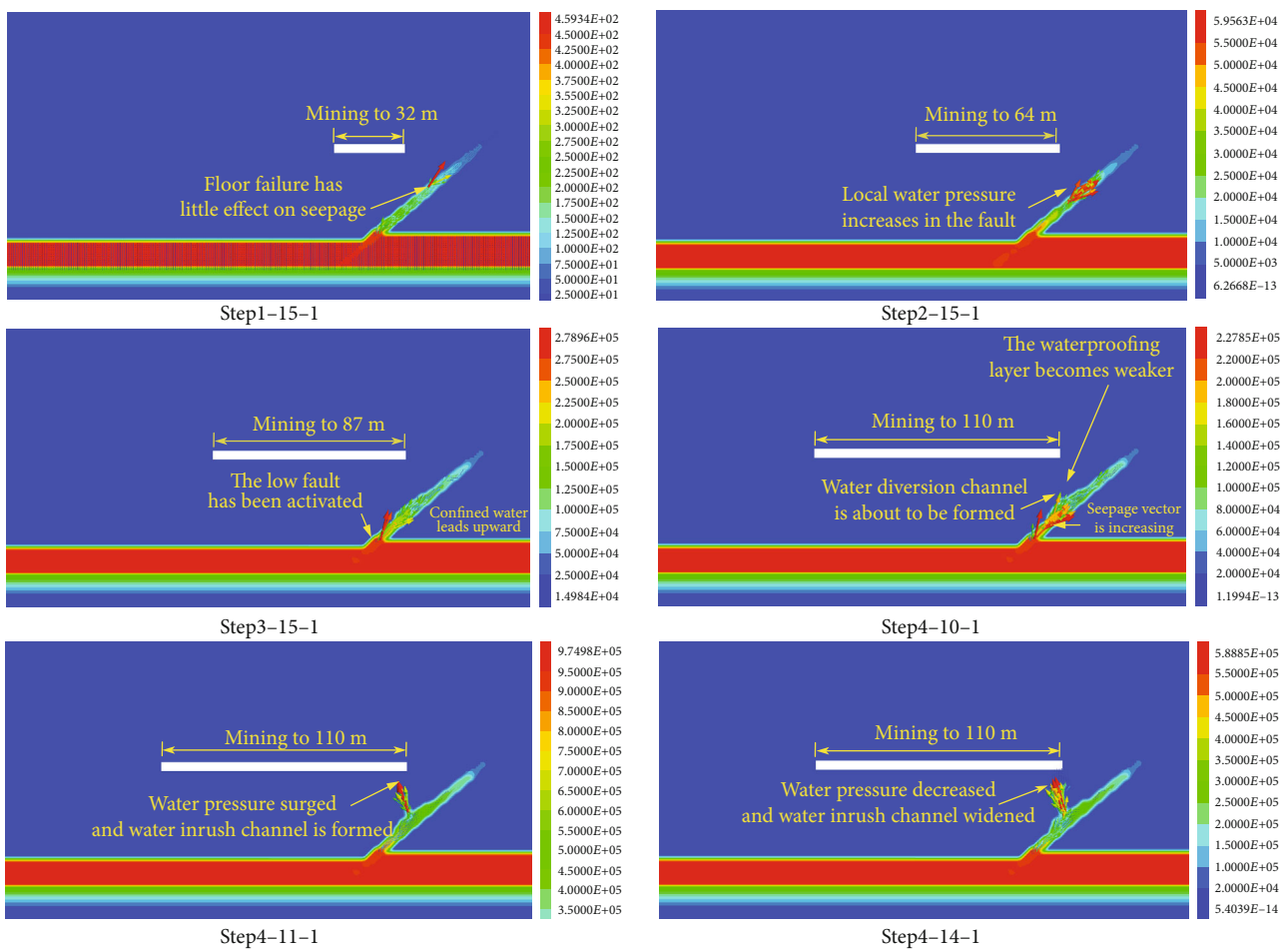

Figure 10: Seepage field evolution diagram.

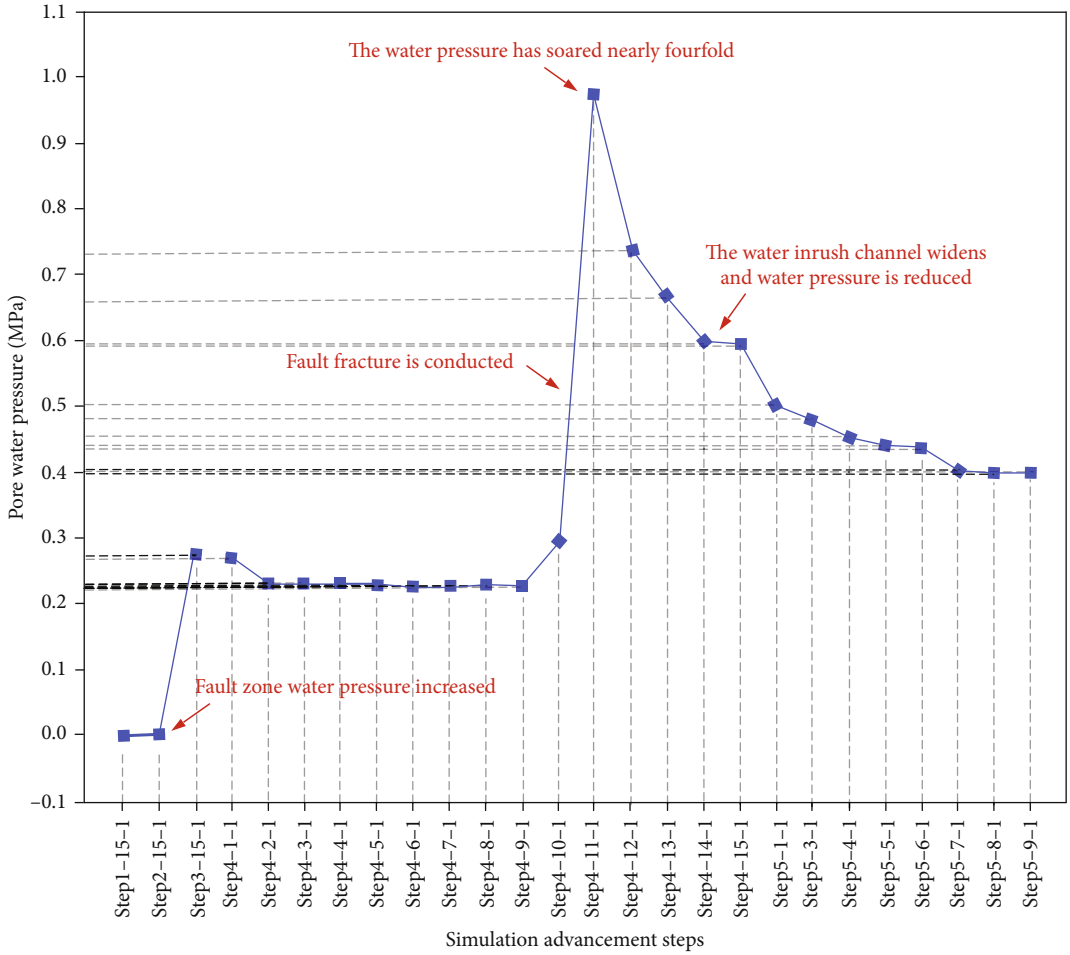

Figure 11: Diagram of the variation of pore water pressure with the advance of the working face.

of 1.4 MPa was applied at the bottom to simulate the effect of Ordovician ash confined water on the floor. The original rock stress was a static stress field, and the rock stratum was a continuous medium. As shown in Figure 7, the fault of the model was normal with a distance of 28 m from the right fault (along the coal seam) and 334 m from the left boundary. By mining from right to left, there were a total of 10 steps. For the first and second steps of mining, each step was 32 m. For the third step to the tenth step, each step was 23 m, for a total of 248 m.

4.1.3. Analysis of Simulation Results of the Plastic Zone. When the working face was mined up to 32 m (step 1-15-1), plastic failure on both sides of the goaf was almost symmetrically distributed (Figure 8). The direct roof and floor mainly experienced tensile failure, and the coal and rock masses on both sides of the goaf mainly experienced shear failure. At this time, the floor fault was almost unaffected by mining disturbance, and only local shear failure occurred inside the fault. As the working face continued advancing to 64 m (step 2-15-1), the plastic failure range of the roof and floor continued expanding and deepening. The plastic failure area was formed in the fault zone due to mining failure of the floor. Subsequently, in the process of advancing to 110 m, the plastic failure range and depth of roof and floor of goaf continued increasing, and the fault continued activating. When advancing to 110 m (step 4-11-1), the cracks between the floor mining failure zone and the pressurized water uplift zone penetrated, resulting in water inrush from the floor.

4.1.4. Analysis of Simulation Results of the Stress Field. The picture shows the variation law of the vertical stress field (Figure 9). With the continuous advancement of the working face, the stress variation range of the cutting side was larger than that of the mining face, resulting in stress concentration on the cutting side. In the process of advancing to 110 m (step 4-15-1), it was evident that the stress on the left side of the fault continued to decrease due to failure of floor mining. Plastic failure occurred when the stress range exceeded the strength of the rock mass. This provided a water inrush channel for the confined water lift.

4.1.5. Analysis of Seepage Field Simulation Results. By combining Figures 10 and 11, it can be seen that the pore water pressure in the fault increases slightly with the advancement of the working face to 64 m (step 2-15-1). Subsequently, when the working face advanced to 110 m (step 4-5-1), the fault zone was activated by disturbance and damage along the fault and confined water pressure continued to increase

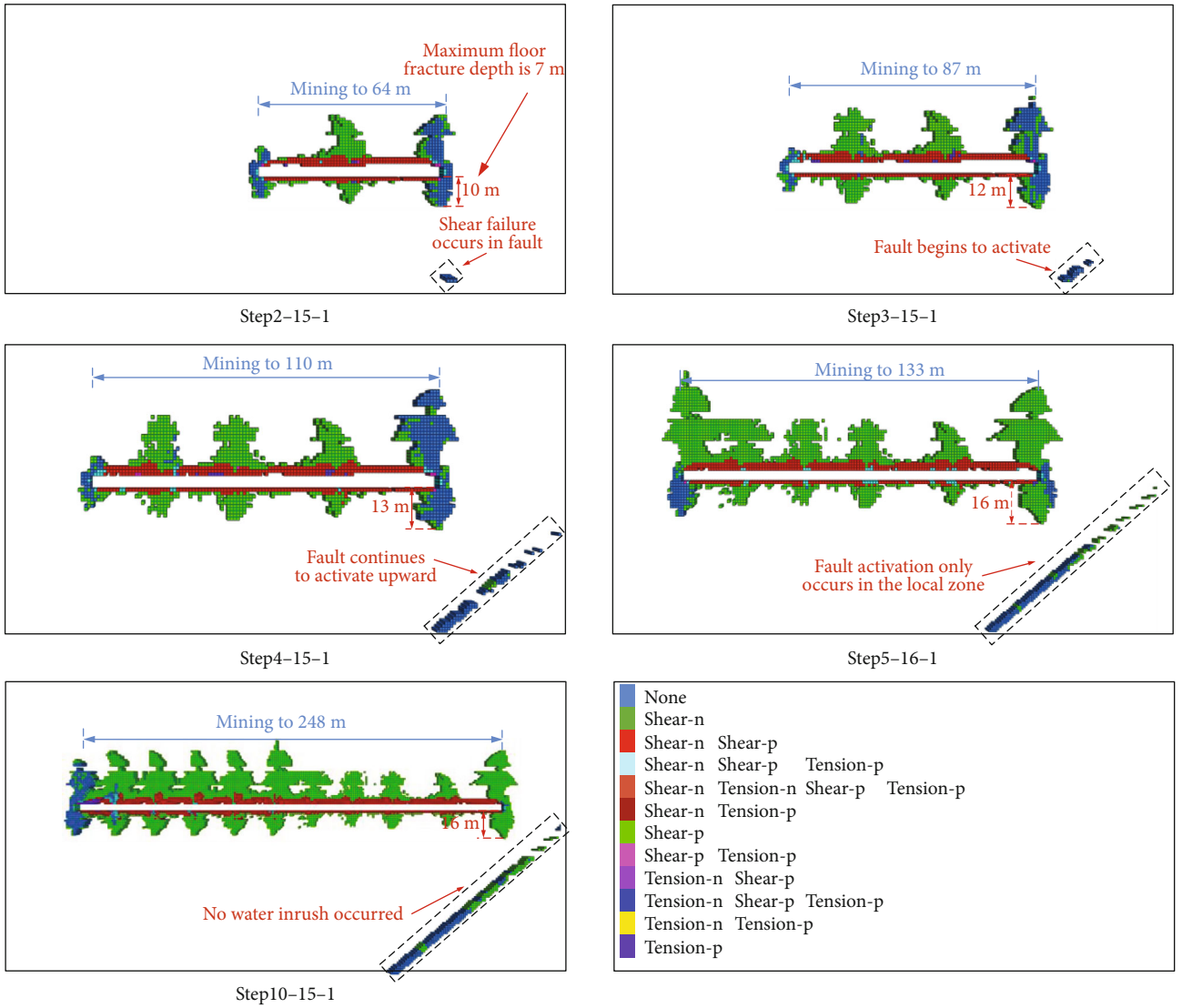

Figure 12: Plastic zone evolution law diagram.

and rose along the fault zone. When the simulation reached step 4-10-1, the development degree of the floor crack and the seepage vector near the mining failure area of the fault zone continued to increase. Until simulation to step 4-11-1, the cracks between the floor mining failure zone and the confined water guide zone developed and led to water inrush channels. The seepage vector in the water inrush channel was huge, and the water pressure increased sharply from the previous 0.23 MPa to 0.97 MPa. Then, in the process of simulation to step 4-14-1, water pressure decreased gradually and stabilized gradually. The change of water pressure in the fault zone is shown in Figure 11.

4.1.6. Comprehensive Comparison of Simulation and Theoretical Results. It can be seen from the above simulation results that when the 28 m waterproof coal pillar is left, the fault confined water guide zone and floor mining failure zone are connected when the working face advances to 110 m. The rapid increase in seepage pressure leads to the inflow of confined water into the goaf, resulting in water inrush. Therefore, the calculation result of the coal pillar empirical formula for the 23503 working face is smaller than the actual situation. However, the theoretical calculation result is 32 m. Moreover, the normal fault of Dongjiahe is on the right side of the 23503 working face. The secondary fractures and structures of the floor are complicated. According to the theoretical calculation value of waterproof coal pillar with 2-3 times safety factor, the cut hole is arranged at 80 m from the fault.

4.2. Numerical Simulation Study of Waterproof Coal Pillar Width 80 m (Working Condition 2). To verify whether it is reasonable to arrange the cut hole at 80 m away from the fault, a numerical simulation analysis was carried out in the case of setting up an 80 m waterproof coal pillar at the 23503 working face. Model establishment and excavation were similar to the 28 m modeling process of working condition 1. In this simulation, the cut hole is 80 m away from the right fault and 282 m from the left boundary. 10 steps are taken from the right to the left. For the first and second steps,

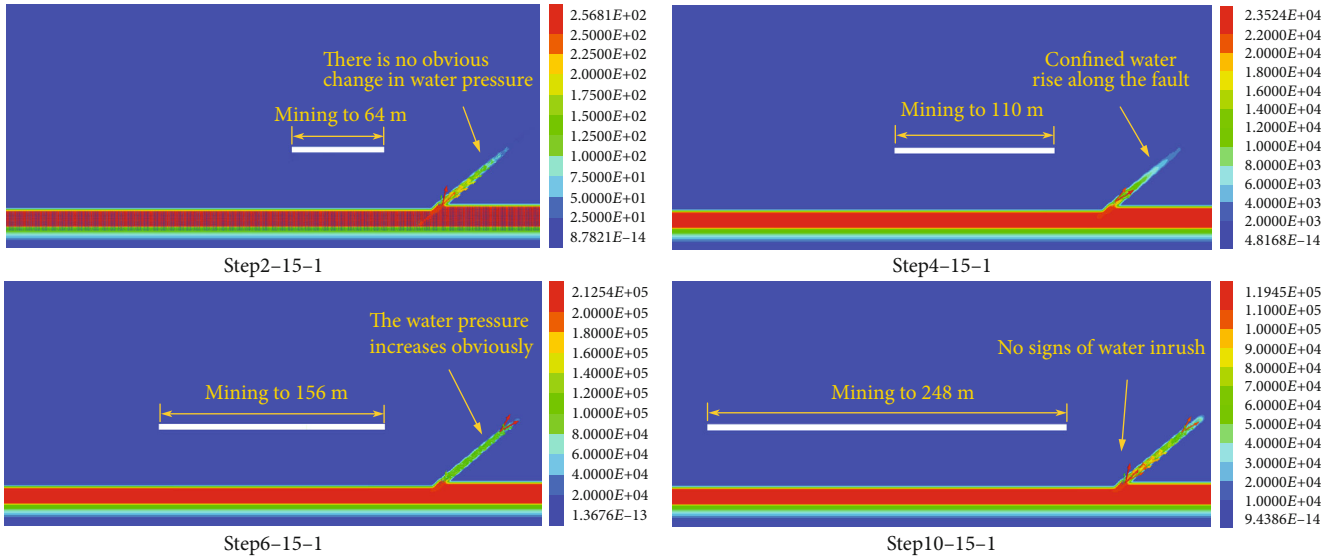

Figure 13: Seepage field evolution diagram.

each mining was 32 m. From the third step to the tenth step, each mining was 23 m and the cumulative mining was 248 m.

4.2.1. Analysis on the Law of the Floor Plastic Zone. As shown in Figure 12, when the working face advanced to 64 m (step 2-15-1), local shear failure occurred at the fault floor under the influence of mining disturbance. Fractures occurred at the interface between the Ordovician ash roof and the fault. When the working face advanced to 110 m (step 4-15-1), the plastic zone of the roof and floor of the mining face expanded. The floor fracture depth on the cut hole side was greater than the floor fracture depth before the working face. At this time, the fault zone was continuously activated upward along the fault. When the working face continued advancing to 133 m (step 5-16-1), the working face reached the limit mining width, and the plastic failure depth of the roof and the floor reached the maximum. At this time, the fault zone was still activated upward along the fault but did not break through the fault zone and hence did not develop outward. When the working face entered the full mining stage until mining was completed, the floor failure depth was less than the maximum failure depth in the nonfull mining stage. Fault activation and confined water uplift only occurred in the fault zone and did not break through the fault zone to develop into the floor mining fracture area.

4.2.2. Analysis on Variation Law of the Floor Seepage Field. As shown in Figure 13, when the working face advanced to 64 m (step 2-15-1), coal seam mining barely affected the change of water pressure in the fault, and high confined water in the floor did not rise along the fault zone. When the working face advanced to 110 m (step 4-15-1), water pressure in the fault changes indicated that the fracture occurred in the fault zone due to the disturbance of floor mining. The confined water was uplifted along the fault zone, and the fault was activated into a water-conducting fault. As the working face continued advancing to 15 6 m (step 6-15-1), Ordovician ash confined water continued to rise upward along the fault zone, and the water pressure in the fault zone reached the maximum value of 0.213 MPa. At this time, the confined water guide zone did not break through the fault zone and therefore did not develop outward. Until the mining of the 248 m (step 10-15-1) working face was completed, the fault activation along the fault zone was higher, and the fracture in the fault zone was more fully developed. However, the confined water does not break through the scope of the fault zone and always moved within the fault zone.

4.2.3. Simulation Result Analysis. From the above simulation results, it can be seen that when an 80 m waterproof coal pillar was left, the floor Ordovician confined water continuously rose along the fault zone. The fault did not extend to the floor mining damage area. The floor mining failure zone was far away from the confined water uplift zone, and no floor water inrush had occurred.

5. Engineering Practice

5.1. Hole Cutting Construction and Groove Wave Detection. Based on the actual situation of the site and through comprehensive research, analysis, and expert meeting to exchange analysis, it was decided that according to the theoretical calculation value of the waterproof coal pillar with 2-3 times safety factor, the cut hole should be arranged at the distance of 80 m from the fault. During the open-cut roadway excavation, three fault structures were revealed, namely, Q1, Q2, and Q3, respectively. Because the Q1 fault was very small and the drop was less than 0.3 m, it did not affect the later excavation. On the other hand, the drops of the roadway where the Q2 and Q3 faults were located were relatively large, and the possible existence of other structures could not be ruled out. Therefore, the groove wave detection was carried out on the working face, and the groove wave observation results are shown in Figure 14.

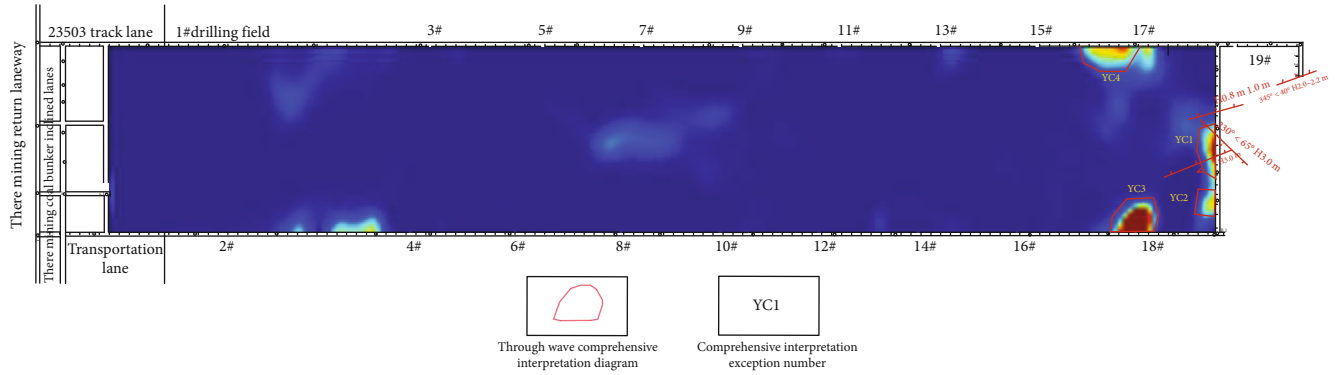

Figure 14: 23503 working face in-seam wave comprehensive interpretation result diagram.

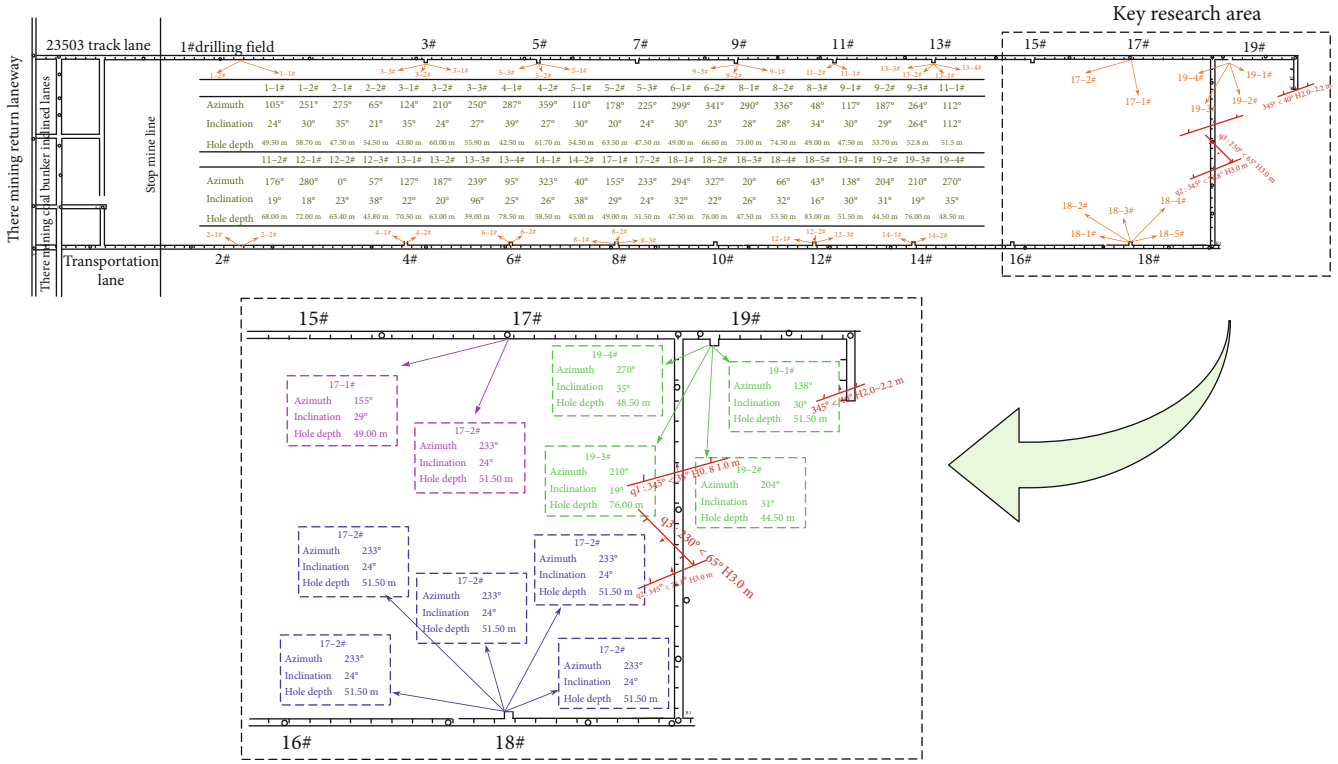

Figure 15: 23503 working face floor drilling and grouting diagram.

The detection results showed that the abnormal area is 30 m from 96 m to 129 m from the track roadway to the transport roadway, 81 m from 1071 m to 1132 m and from 1160 m to 1180 m in the transportation roadway, and 102.3 m from 158 m to 255 m and 1060.6 m to 1066 m in the track roadway. According to detection results, it was estimated that the fault at the cut hole extends to the west for a range of 20 m.

The hydrogeological conditions of the 23503 working face are complex, and the driving areas are all located below the Ordovician ash static water level. These areas belong to the pressure-bearing area. According to drilling data, there are different water gushing degrees in the drilling site. Judging from the amount of water gushing and its static pressure, the gushing water recharge had no hydraulic relationship with the underlying Ordovician limestone solution fissure water. It should be fracture water in the lower aquifer group (K2 quartz sandstone) of coal measure strata. However, it cannot be ruled out that the impact of mining causes Ordovician water to flow into the K2 sandstone layer. This forms a large amount of indirect replenishment to the water inrush source. To not affect the safe mining of the working face, the mine carried on the grouting transformation to the floor K2 sandstone.

5.2. Implementation Scheme and Application Effect of Grouting Reinforcement in the Working Face. There are two roadways in the 23503 working face, which are the transport roadway and track roadway. The length of the two grooves in the transport lane and track lane was 1200 meters, and the cut was 180 meters. There are 13 drilling sites and 39 holes in the working

face. The specific gravity of the grout was between 1.13 and 1.30 g/cm^2, and the total grouting volume was 7970.7 cubic meters (Figure 15). The grouting reinforcement project of the working face starts from 28 November 2018 to 13 October 2019. After completing grouting, the whole working face was explored by the electrical method to meet water prevention and control requirements. Because the Q2 and Q3 faults exposed by the open-cut roadway have not developed to the Ordovician ash roof interface and are coupled with the previous floor grouting transformation, the water inflow of the open-cut roadway was reduced to 20 m^3/h. It met the requirements of the detailed rules of water prevention and control and the existing drainage capacity of 200 m^3/h of the mine. Currently, the 23503 working face has mined 700 m. From the observation data of the underground water inrush point, it can be seen that the average water inflow was maintained at 40-60 m^3/h in the process of mining. The highest water inflow in the whole working face was over 105 m^3/h. However, it still meets the existing drainage capacity of the mine and does not cause a water inrush accident.

6. Conclusions

Based on the plastic slip line field theory, this paper puts forward the analytical solution of the limit width of the waterproof coal pillar. Moreover, this paper analyzed the activation law of floor fault in the 23503 working face of the Dongjiahe coal mine. It also verified the theory by numerical simulation and engineering practice. The conclusions are as follows:

(1) The numerical models under two different conditions of setting coal pillar width were established using the finite difference software. The laws of deformation and failure of the through fault floor and fault activation were obtained. It was determined that the safety width of the waterproof coal pillar is 80 m. This provided more reasonable data than the empirical value mentioned in the "coal mine safety regulations" for the location of new cut holes

(2) When the waterproof coal pillar was set at 28 m, the existence of the through fault hindered the transmission of mining stress in the floor. This made the stress concentration in the floor rock mass between the goaf and the fault to increase, thereby deepening the floor failure depth near the fault. With the advancement of the working face, the fault zone continued to activate upward, and the seepage vector in the zone continued to grow and gradually extended to the failure depth of the floor

(3) In the practical application of the research results, three fault structures were exposed during the process of open-hole excavation. Combining these results with grooving wave detection results in the 23503 working face, grouting transformation was carried out on the working face floor. This measure reduced the risk of floor water inrush and had a good effect of preventing water inrush. It also provided engineering references and practical experiences for water disaster prevention and for the control of structural floors under similar conditions in the Weibei mining area for future benefits

Data Availability

Some or all data, models, or codes generated or used during the study are available from the corresponding author by request.

Conflicts of Interest

The authors declare that there is no conflict of interest regarding the publication of this paper.

Acknowledgments

The authors are grateful for the financial assistance provided by the Open Projects of Key Laboratory of Coal Resources Exploration and Comprehensive Utilization, Ministry of Land and Resources (KF2020-5); the National Natural Science Foundation of China (Nos. 41402265 and 51874229); and the Natural Science Foundation of Shaanxi Province (2020JZ-52).

References

[1] A. Li, *Research on Mechanism and Application of Coal Seam Floor Failure over a Confined Water Body in Weibei Coalfield*, Chinese University of Mining and Technology Press, XuZhou, 2015.

[2] A. Li, Q. Ma, Y. Q. Lian, L. Ma, Q. Mu, and J. B. Chen, "Numerical simulation and experimental study on floor failure mechanism of typical working face in thick coal seam in Chenghe mining area of Weibei, China," *Environmental Earth Science*, vol. 79, no. 5, article 8839, 2020.

[3] X. G. Meng, W. T. Liu, and D. R. Mu, "Influence analysis of mining's effect on failure characteristics of a coal seam floor with faults: a numerical simulation case study in the Zhaolou coal mine," *Mine Water Environment*, vol. 37, no. 4, pp. 754–762, 2018.

[4] S. H. Dong, H. Wang, and W. Z. Zhang, "Judgement criteria with utilization and grouting reconstruction of top Ordovician limestone and floor damage depth in North China coal field," *Journal of China Coal Society*, vol. 44, pp. 2216–2226, 2019.

[5] Q. Wu and M. Wang, "Characterization of water bursting and discharge into underground mines with multilayered groundwater flow systems in the North China coal basin," *Hydrogeology Journal*, vol. 14, no. 6, pp. 882–893, 2006.

[6] A. Li, Q. Mu, W. Zhang, C. Y. Liu, F. Wang, and L. Mou, "Research on a numerical simulation and prediction model of floor mining failure depth in the Chenghe mining area," *Geofluids*, vol. 2020, Article ID 8850156, 14 pages, 2020.

[7] W. B. Sun, S. H. Zhang, W. J. Guo, and W. T. Liu, "Physical simulation of high-pressure water inrush through the floor of a deep mine," *Mine Water Environment*, vol. 36, no. 4, pp. 542–549, 2017.

[8] S. Zhang, W. Guo, Y. Li, W. Sun, and D. Yin, "Experimental simulation of fault water inrush channel evolution in a coal mine floor," *Mine Water Environment*, vol. 36, no. 3, pp. 443–451, 2017.

[9] A. Li, Q. Ma, K. Li, and L. Li, "Evaluation on floor water inrush danger of Weibei during mining over pressurized water and prevention countermeasures to the water disaster," *Journal of Mines, Metals and Fuels*, vol. 66, no. 4, pp. 231–244, 2018.

[10] K. Ma, X. Y. Sun, C. A. Tang, F. Z. Yuan, S. J. Wang, and T. Chen, "Floor water inrush analysis based on mechanical failure characters and microseismic monitoring," *Tunnelling and Underground Space Technology*, vol. 108, article 103698, 2021.

[11] Y. Zhang, "Mechanism of water inrush of a deep mining floor based on coupled mining pressure and confined pressure," *Mine Water Environment*, vol. 40, no. 2, pp. 366–377, 2021.

[12] L. J. Donnelly, "A review of coal mining induced fault reactivation in Great Britain," *Quarterly Journal of Engineering Geology and Hydrogeology*, vol. 39, no. 1, pp. 5–50, 2006.

[13] W. K. Bu and X. B. Mao, "Research on effect of fault dip on fault activation and water inrush of coal floor," *Chinese Journal of Rock Mechanics and Engineering*, vol. 21, pp. 119–123, 2009.

[14] H. Pu and J. Zang, "Numerical simulation of water inrush from coal roof affected by fault," *Journal of Mining and Safety Engineering*, vol. 27, no. 3, pp. 421–424, 2010.

[15] X. J. Hu, W. P. Li, D. T. Cao, and M. C. Liu, "Index of multiple factors and expected height of fully mechanized water flowing fractured zone," *Journal of Mining and Safety Engineering*, vol. 37, no. 4, pp. 613–618, 2012.

[16] Q. Wu, J. J. Shen, W. T. Liu, and Y. Wang, "A RBFNN-based method for the prediction of the developed height of a water-conductive fractured zone for fully mechanized mining with sublevel caving," *Arabian Journal of Geosciences*, vol. 10, no. 7, article 2959, 2017.

[17] L. W. Chen, X. Q. Feng, D. Q. Xu, W. Zeng, and Z. Y. Zheng, "Prediction of water inrush areas under an unconsolidated, confined aquifer: the application of multi-information superposition based on GIS and AHP in the Qidong coal mine, China," *Miner Water Environment*, vol. 37, no. 4, pp. 786–795, 2018.

[18] A. Li and K. Li, "Floor water inrush risk evaluation for mining above confined aquifer in no. 5 coal seam of Taiyuan Group at Dongjiahe coal mine," *Electronic Journal of Geotechnical Engineering*, vol. 21, pp. 1809–1822, 2016.

[19] H. Y. Yin, J. C. Wei, L. Lefticariu et al., "Numerical simulation of water flow from the coal seam floor in a deep longwall mine in China," *Mine Water and the Environment*, vol. 35, no. 2, pp. 243–252, 2016.

[20] V. N. Odintsev and N. A. Miletenko, "Water inrush in mines as a consequence of spontaneous hydrofracture," *Journal of Mining Sciences*, vol. 51, no. 3, pp. 423–434, 2015.

[21] X. Y. Wang, T. T. Wang, Q. Wang, X. M. Liu, R. Z. Li, and B. J. Liu, "Evaluation of floor water inrush based on fractal theory and an improved analytic hierarchy process," *Mine Water and the Environment*, vol. 36, pp. 87–95, 2018.

[22] R. Álvarez, A. Ordóñez, E. de Miguel, and C. Loredo, "Prediction of the flooding of a mining reservoir in NW Spain," *Journal of Environmental Management*, vol. 184, Part 2, pp. 219–228, 2016.

[23] J. H. Guo, L. Q. Ma, and D. S. Zhang, "Management and utilization of high-pressure floor-confined water in deep coal mines," *Mine Water and the Environment*, vol. 38, no. 4, pp. 780–797, 2019.

[24] S. H. Yuan and G. L. Han, "Combined drilling methods to install grout curtains in a deep underground mine: a case study in Southwest China," *Mine Water and the Environment*, vol. 39, no. 4, pp. 902–909, 2020.

[25] Q. Wang, Q. Qin, B. Jiang, H. C. Yu, R. Pan, and S. C. Li, "Study and engineering application on the bolt-grouting reinforcement effect in underground engineering with fractured surrounding rock," *Tunnelling and Underground Space Technology*, vol. 84, pp. 237–247, 2019.

[26] H. Shi and J. Zhang, "Accurate directional water detection and water release technology for underground coal mine," *Safety in Coal Mine*, vol. 46, pp. 64–67, 2015.

[27] J. Q. Jia, H. T. Wang, G. Z. Hu, X. H. Li, and Z. G. Yuan, "Methods of retaining water barrier and its stability analysis of steep working face," *Journal of China Coal Sociaty*, vol. 34, pp. 315–319, 2009.

[28] A. Li, "Water inrush mechanism on seepage and stress coupling damage of coal floor under water pressure and its engineering application," *Xi'an University of Science and Technology*, 2012.

[29] X. N. Zhang, M. Wang, and J. Y. Fan, "Study on mechanism and countermeasures of broken floor heave in mining roadway," *Safety in Coal Mines*, vol. 50, pp. 197–202, 2019.